

10. SITE 1214¹

Shipboard Scientific Party²

PRINCIPAL RESULTS

Background

Site 1214 is located at 3402 m water depth on the southern flank of the Southern High of Shatsky Rise. The site is at the location of Deep Sea Drilling Project (DSDP) Site 306 (Larson, Moberly, et al., 1975). At Site 306, 475 m of sedimentary rocks was penetrated with rotary core barrel (RCB) drilling but only continuously cored from 207.5 m to total depth. Most of the upper section (28 to 207.5 meters below seafloor [mbsf]) was alternately cored and washed at ~9-m intervals. The recovery was ~7%. The recovered sedimentary rocks, mainly calcareous porcellanite and chert with minor nannofossil chalk and ooze are late Albian to early Berriasian in age, covered by ~9 m of Holocene siliceous foraminifer-bearing nannofossil ooze.

According to the coring record from Site 306 (Larson, Moberly, et al., 1975), the uppermost Cretaceous sediments lie between Reflectors R1 and R2 of Sliter and Brown (1993). Reflector R1 (Cenomanian/Turonian boundary) crops out a few kilometers northeast of Site 306. Reflector R2 of Barremian/Aptian boundary age corresponds to the top of the porcellanite, chert, and shale section at Site 306 that rests on basement. The interval between R1 and R2 consists of chalk, chert, and porcellanite.

Site 1214 lies in the middle of the mid-Cretaceous portion of the Shatsky Rise depth transect between Site 1207 (3101 m) and Site 1213 (3883 m). The objective at Site 1214 was to recover a more complete and continuous record of the Site 306 sequence. As part of the Shatsky Rise mid-Cretaceous depth transect, drilling at Site 1214 addresses a number of leg-related objectives concerning ocean circulation and environmental change in an interval of global warmth.

¹Examples of how to reference the whole or part of this volume.

²Shipboard Scientific Party addresses.

Summary of Results

Hole 1214A was cored with RCB drilling terminating at 235.9 mbsf in the Hauterivian. Average recovery of 7% was equivalent to Site 306. The sedimentary section is divided into units based on composition and color. Lithologic Unit I (Holocene to Pleistocene; 0.0–6.9 mbsf) consists of very pale yellowish brown to moderate yellowish brown clayey foraminiferal nannofossil ooze and very pale to moderate yellowish brown clayey nannofossil ooze with foraminifers. Subunit IIA (late Albian; 6.9–34.5 mbsf) is composed of moderate yellowish brown to light olive-gray chert and very light gray to yellowish gray porcellanite, with minor white nannofossil chalk. Medium dark gray, dark gray to grayish black chert, and very light gray to light greenish gray porcellanite are grouped in Subunit IIB (late Albian to early Albian; 34.5–110.7 mbsf). Very light to light greenish gray limestone with radiolarians is a minor lithology in this subunit. Subunit IIC (early Albian to late Aptian; 110.7–207.0 mbsf) contains medium dark gray, dark gray, brownish gray, grayish brown, and moderate brown chert, and yellowish gray, very light to light greenish gray porcellanite. Olive-black, greenish black, and dark greenish gray claystone to clayey porcellanite is placed in Subunit IID (early Aptian; 207.0–216.6 mbsf). Finally, Subunit IIE comprises brownish gray, brownish black, and olive-black chert and light greenish gray, greenish gray, and yellowish gray porcellanite (Hauterivian; 216.6–235.9 mbsf). Throughout the section, porcellanite and limestone have variable amounts of radiolarians and nannofossils. Most of the ages were obtained from chalk adhered to the sides of chert fragments. This sediment indicates the soft and relatively unaltered nature of the unrecovered intervals.

Highlights

The results of coring at Site 1214 provide important information on the stratigraphy of the mid-Cretaceous section on Shatsky Rise. The interpreted stratigraphy of Site 1214 is different from the stratigraphy of Site 306 from Larson, Moberly, et al. (1975) and Sliter (1992). One possibility for this difference is that Site 1214 is actually located at a distance from Site 306, given the imprecision of the coordinates of the latter site. A second possibility is that the biostratigraphy of Site 306 was conducted almost exclusively using planktonic foraminifers, whereas that of Site 1214 included nannofossils and radiolarians.

Site 1214 has an expanded Albian section, ~180 m in thickness, compared to 120–130 m at Site 1213. One possible reason for this disparity is that the latter site is located at greater water depth and thus subject to greater dissolution. More significantly, the stratigraphy of Site 1214 confirms that much of the Barremian corresponds to a regional unconformity on the southern part of Shatsky Rise. In both locations, lower upper Hauterivian sedimentary rocks are found in the core below lower Aptian horizons. At Site 1213, one sample at the top of Core 198-1213B-9R contained neither Aptian nor Hauterivian markers. Even with this uncertainty, combined data from Sites 1213 and 1214 suggest that a significant hiatus occurred during much of the Barremian and at least part of the upper Hauterivian. The reason for this unconformity is currently unclear. This interval was present at Site 1207, which was some 800 m shallower than Site 1213 at that time; thus, a temporary change in the calcite compensation depth (CCD) could have led to the hiatus. However, the Barremian in most parts of the ocean, including the Pa-

cific, is generally regarded as an interval when the CCD was relatively deep (i.e., Thierstein, 1979). Thus, it is possible that this interval corresponded to an erosional event that removed sediment from the flanks of the Southern High and not from the top of the Northern High.

The lower Aptian section in Hole 1214A (Section 198-1214A-23R-1) contains olive-black, greenish black, and dark greenish gray claystone to clayey porcellanite. Both of these lithologies are laminated in places, indicating low-oxygen conditions on the seafloor. Organic carbon (C_{org}) contents are low (<0.5 wt%) in the greenish gray lithologies. Four thin, discrete bentonite or tuff layers are observed within pieces of porcellanite. A sample from a piece of olive-black claystone toward the top of Section 198-1214A-23R-1 contains 1.4% C_{org} . Characterization of the organic matter from this sample indicates that it is algal and bacterial in origin, similar to highly carbonaceous lower Aptian lithologies from Sites 1207 and 1213 (see “**Geochemistry**,” p. 61, in “Specialty Syntheses” in the “Leg 198 Summary” chapter). This interval lies in nannofossil Zone NC6, between the first occurrences (FOs) of *Eprolithus floralis* and *Hayesites irregularis*. Most of the sedimentary rocks in Section 198-1214A-23R-1 are noncalcareous but contain abundant radiolarians in discrete layers. Diagnostic radiolarian faunas in these levels are similar to assemblages observed in the Livello Selli in the Cismon core from the southern Alps of Italy (Premoli Silva et al., 1999) and in horizons bounding organic-rich intervals in the lower Aptian at Site 1213 (see “**Biostratigraphy**,” p. 56, in “Specialty Syntheses” in the “Leg 198 Summary” chapter). Thus, combined biostratigraphic and lithostratigraphic evidence suggests that the olive-black claystone comes from within the general Aptian Oceanic Anoxic Event (OAE1a) interval, but certainly not from near the peak of the event as did samples with much higher C_{org} contents from Sites 1207 and 1213.

BACKGROUND AND OBJECTIVES

Site 1214 is located in lower bathyal (3402 m) water depth on the southern flank of the Southern High of Shatsky Rise at the location of DSDP Site 306 (Larson, Moberly, et al., 1975). At Site 306, 380.6 m of 475 m drilled was cored, but a total of only 27.3 m (7%) was recovered. These sedimentary rocks include calcareous porcellanite and chert with subordinate nannofossil chalk and ooze ranging in age from late Albian to early Berriasian. The Cretaceous sequence is overlain by a thin (9 m) Holocene ooze cover. The biostratigraphy of Site 306 was reinterpreted by Sliter (1992), who also reinterpreted the seismic stratigraphy (Sliter and Brown, 1993). R2, the shallowest reflector in the sequence, corresponds to the Barremian/Aptian boundary.

Site 1214 is the second deepest site in the Shatsky Rise transect, ~500 m deeper than Site 1211 and ~450 m shallower than Site 1213. The Site 1214 depth is close to that of Site 1208 on the Central High. The depth lies in the middle of the three sites targeting mid-Cretaceous sediments, including Site 1207 (3101 m) and Site 1213 (3883 m). According to the paleodepth reconstruction of Thierstein (1979), the site lay at ~2.2 km at 120 Ma, assuming normal oceanic crust subsidence. However, subsidence was likely more rapid than normal crust in the interval immediately after its formation; thus, the site may have been slightly deeper.

Coring at Site 1214 was designed to recover a more complete and continuous record of the Hole 306 sequence. The major goals of Site 1214 drilling were to core an intermediate-water Aptian–Albian se-

quence, improving on the Site 306 recovery. This section exists at shallow burial depths; thus, it can be reached without coring through an extensive ooze-chert sequence. The site will be included in broad leg-based objectives that include

1. Recovering organic-rich sediments suitable for detailed paleontological and geochemical investigations that can be used to constrain the response of marine biotas to mid-Cretaceous Oceanic Anoxic Events (OAEs) and to determine changes in carbon and nutrient cycling. In addition, the Shatsky transect will allow us to evaluate whether the pattern of organic-rich sediments conforms to an oxygen minimum zone model or to a deep basinal model.
2. Determining fluctuations in the CCD through the mid-Cretaceous, comparing them to other records from the North Pacific as well as from other ocean basins, and interpreting them in a paleoceanographic framework.
3. Relating changes in biotic assemblages through time to environmental changes.

OPERATIONS

Transit from Site 1211 to Site 1214

The 22-nmi transit to Site 1214 took 2.5 hr at an average speed of 8.8 kt. At 0420 hr on 12 October, the ship was switched over to dynamic positioning mode, initiating operations at Site 1214.

Site 1214

Hole 1214A

An RCB bottom-hole assembly was tripped to the seafloor, and the bit tagged bottom at 3413.0 meters below rig floor, or 3401.6 meters below sea level. RCB coring advanced the hole from the seafloor to 235.9 mbsf before coring time expired for the leg. Chert was encountered in drilling the first core and continued throughout the hole, which is reflected in the poor overall recovery (7%) (Table T1). The drill string was retrieved while the usual end-of-leg maintenance and inspections were performed. At 0025 hr on 15 October 2001, the bit cleared the rig floor, ending operations at Site 1214.

Transit from Site 1214 to Honolulu, Hawaii

After securing the ship for transit, we departed Site 1214 for port at 0030 hr on 15 October. The 2500-nmi transit to Honolulu, Hawaii, took 9.85 days at an average speed of 10.75 kt. At 2100 hr on 23 October, the first line was ashore, officially ending Leg 198.

LITHOSTRATIGRAPHY

Description of Lithologic Units

Site 1214 lies on the southwest flank of Shatsky Rise at a depth of 3402 m and is a revisitation of Site 306. Rotary coring down to 235.9

T1. Coring summary, p. 26.

mbsf at Site 1214 recovered 15.2 m of sediment and sedimentary rock. The sediment is divided into two lithologic units (Fig. F1). Unit I, extending from 0.0 to 6.9 mbsf, is composed of Holocene to Pleistocene sediments. Unit I recovery was 1.32 m (19%). This unit consists of clayey foraminiferal nannofossil ooze to clayey nannofossil ooze with foraminifers. Unit II consists of chert, lithified, porous, calcareous porcellanite, and minor chalk of late Albian to Hauterivian age. Unit II recovery averaged 7%.

Lithologic Unit I

Interval: 198-1214A-1R-1, 0 cm, through 1R-1, 27 cm (unit defined to correspond to cored interval)
 Depth: 0.0 to 6.9 mbsf
 Age: Holocene to Pleistocene

Lithologic Unit I consists of pale to moderate yellowish brown (10YR 6/2 to 10YR 5/4) clayey foraminiferal nannofossil ooze underlain by very pale orange (10YR 8/2) to moderate yellowish brown (10YR 5/4) clayey nannofossil ooze with foraminifers. Carbonate content is 60 to 65 wt%, of which 40%–45% is nannofossils and 20%–25% is foraminifers. Clay content ranges between 25% and 30%, and there are minor percentages of quartz, feldspar, volcanic glass, and Fe oxides. The unit also contains pumice clasts and well-preserved pyrite-filled burrows. Bioturbation is moderate throughout the unit. The boundary between Units I and II corresponds to a Pleistocene to upper Albian unconformity.

Lithologic Unit II

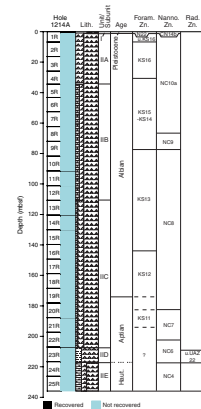
Interval: 198-1214A-2R-1, 0 cm, through 25R-1 (end of hole)
 Depth: 6.9 to 235.9 mbsf
 Age: late Albian to Hauterivian

Lithologic Unit II consists primarily of fragments (drilling breccia) of chert and porous calcareous porcellanite. Chert usually occurs as irregular-shaped fragments of different colors but is also present as blebs and small stringers in the porcellanite. Porcellanite of various colors (depending on carbonate and clay content) exists as fragments and coatings or inclusions in the chert. Nannofossil claystone, limestone with radiolarians, and nannofossil chalk are present in minor amounts. This unit has been divided into five subunits that are generally based on the color of the chert (Table T2) and changes in the microfossil assemblage composition.

Subunit IIA

Subunit IIA (interval 198-1214A-2R-1 through 4R-1; 6.9 to 34.5 mbsf) consists of rare to moderate bioturbated, moderate yellowish brown (10YR 5/4) to light olive gray (5Y 6/1) chert and very light gray (N8) to yellowish gray (5Y 8/1) porcellanite. Minor fragments of white (N9) nannofossil chalk are also present. Porcellanite is present as fragments as well as coatings on and inclusions in the chert. Contacts between the chert and porcellanite are irregular and sometimes patchy. Radiolarians (often replaced by calcite) and foraminifers are present in both chert and porcellanite.

F1. Core recovery, lithologic units, and age with corresponding biostratigraphic zonation, p. 18.



T2. Downhole variation in chert colors, Hole 1214A, p. 27.

Subunit IIB

In Subunit IIB (interval 198-1214A-5R-1 through 12R-1; 34.5 to 110.7 mbsf) the chert is medium dark gray (N4) and dark gray (N3) to grayish black (N2), whereas the porcellanite is very light gray (N8) to light greenish gray (5GY 8/1). In Sections 198-1214A-11R-1 through 12R-1, the chert color becomes more brownish (brownish gray, 5YR 4/1, to grayish brown, 5YR 3/2), and very light to light greenish gray (5GY 8/1–9/1) limestone with radiolarians is present. Contacts between limestone and chert are gradational, usually with porcellanite in between. Chalk is only present as coatings and inclusions in the chert in this subunit. The degree of bioturbation is rare to moderate. In Section 198-1214A-5R-1, 14 cm, the nannofossil chalk has streaks of purplish gray minerals identified in smear slides as chalcedony. Chalcedony was also found at Site 306 in chert fragments and former radiolarian molds.

Subunit IIC

The dominant lithology within Subunit IIC (interval 198-1214A-13R-1 through 22R-1; 110.7 to 207.0 mbsf) is medium dark gray (N4), dark gray (N3), brownish gray (5YR 4/1), grayish brown (5YR 3/2), and moderate brown (5YR 3/4) mottled chert, both with and without visible radiolarians. Porcellanite is still present, but it is yellowish gray (5Y 8/1) and very light to light greenish gray (5GY 8/1–9/1) in this subunit. It ranges in composition from porcellanite with radiolarians to nannofossil porcellanite with radiolarians to radiolarian nannofossil porcellanite. Porcellanite forms coatings on or inclusions in chert. White (N9) nannofossil chalk also is present in this subunit as burrow fill and inclusions. Bioturbation is rare to moderate. Downcore in Subunit IIC, the porcellanite begins to exhibit vague, wavy lamination. In some samples, the lamination drapes over small nodules of incipient chert or porcellanite, indicating that compaction occurred during or after the formation of chert. From Core 198-1214A-14R downward, radiolarians occasionally are replaced or infilled with pyrite. In Cores 198-1214A-16R and 18R, pyrite is present as compressed, millimeter-scale microlayers.

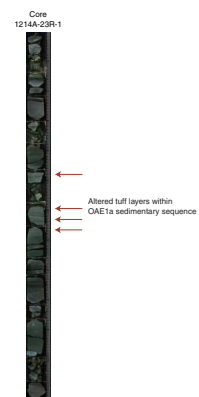
Subunit IID

Subunit IID (Section 198-1214A-23R-1; 207.0 to 216.6 mbsf) consists mainly of olive black to greenish black (5G 2/1) and dark greenish gray (5G 4/1) claystone to clayey porcellanite. Minor amounts of greenish gray (5G 6/1) to dark greenish gray (5G 4/1) porcellanite with local concentrations of radiolarians are present. The sediment is finely laminated, and darker-colored lamina commonly contain pyrite. Several gray (N5), centimeter-thick horizons, which appear to be altered fine tuffs, are interbedded with the porcellanite and claystone. These layers occur at 48–49, 59–60, 63–64, and 66–67 cm. The contacts between gray layers and the surrounding greenish gray claystone and porcellanite are sharp and horizontal (Fig. F2). The boundary between Subunits IID and IIE is placed at the lower Aptian to Hauterivian unconformity.

Subunit IIE

The fifth and final subunit recovered at Site 1214, Subunit IIE, extends from Section 198-1214A-24R-1 through Section 25R-1 (216.6 to 235.9 mbsf). The apparent subunit stratigraphy progresses from light greenish gray (5GY 8/1), greenish gray (5GY 6/1), and yellowish gray (5Y 8/1) porcellanite at the top to brownish gray (5YR 4/1), brownish black (5YR 2/1), and olive-black (5Y 2/4) chert with or without radiolarians.

F2. Sedimentary sequence spanning OAE1a, p. 19.



However, drilling disturbance and poor recovery preclude reconstructing the absolute piece-by-piece orientation and stratigraphy. Minor amounts of light greenish gray (5GY 8/1) nannofossil chalk are present in Core 198-1214A-25R. Both chalk and porcellanite are present as coatings on the chert, and the chalk has subhorizontal streaks of pyrite.

Interpretation

Unit I

Core recovery of Unit I was poor (19%) compared to Site 306, where recovery was 94%. The unit consists of Pleistocene sediments that unconformably overlie upper Albian sediments of Unit II. This unconformity is similar in duration to the major unconformities found at the other relatively deep sites cored during Leg 198. However, the location of Site 1214 (and Site 306) on the flank of a submarine canyon suggests that much of the hiatus is attributable to erosion associated with the cutting of this canyon.

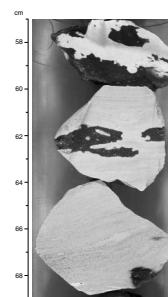
Unit II

The poor recovery of Unit II was due to abundant chert and porcellanite, resulting in the preferential loss of softer sediments during coring. The primary record of less-indurated carbonate sediments is derived from irregular surfaces and inclusions where it was not completely washed or scraped away. An unconformity is present in Unit II (between Sections 198-1214A-23R-1 and 24R-1), where Barremian sediments are absent. This might be due to deep currents sweeping the flanks of Shatsky Rise or poor recovery. Deposition of Unit II sediment occurred above the CCD, except for Core 198-1214A-23R, based on the presence of carbonate (chalk, calcareous porcellanite, and limestone) throughout the unit.

The goal of returning to DSDP Site 306 to core Site 1214 was to recover C_{org} -rich sediments corresponding to Cretaceous OAE1a (the Selli-equivalent black shale deposit) at an intermediate paleowater depth between Sites 1207 and 1213. The OAE1a sequence was inferred to have been present at Site 306 (Section 32-306-13-CC) as an interval of grayish olive-green laminated porcellanite with a thin layer of black, carbonaceous, silicified radiolarian claystone. A similar sedimentary sequence was recovered in Core 198-1214A-23R, characterized by primarily greenish gray radiolarian-rich porcellanite and claystone that was burrowed and mottled at the top of the core and then laminated within the middle of the short recovered sequence, followed by an interval of distinctly burrowed claystone and porcellanite below. Pyrite is present as burrow fill throughout the core. Of particular interest is the presence of several gray, centimeter-thick horizons that appear to be altered fine tuffs (198-1214A-23R-1, 48–49, 59–60, 63–64, and 66–67 cm). The contacts between these gray layers and the surrounding greenish gray claystone and porcellanite are sharp and horizontal (Fig. F2).

Abundance of silica-rich lithologies probably reflects high production of siliceous biogenic material, most likely related to the equatorial position of Shatsky Rise during most of the Cretaceous. In Subunit IIC and downcore, radiolarians have in some intervals been replaced by pyrite (Fig. F3). This indicates a more sulfide-rich, reducing environment possibly related to higher productivity.

F3. Pyrite that has replaced radiolarians, p. 20.



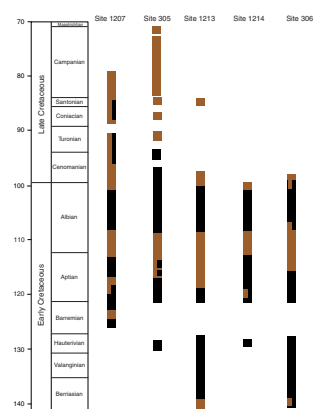
Porcellanite and chalk in Subunits IIC through IIE are faintly laminated in some intervals. The lamination may have resulted from burrow flattening during sediment burial and compaction. However, some burrows in the cherts have been preserved without being flattened. This can also be seen at Site 1213 and is evidence for relatively early silica cementation.

In Subunit IIA, and to some extent in Subunit IIC, the chert is often brownish, and the porcellanite a more yellowish to olive gray color (Table T2). Chert in Subunits IIB and IIE is more black hued, and porcellanite records different shades of greenish gray. Subunit IID consists of dark greenish gray- to greenish black-colored porcellanite, claystone, and clayey porcellanite. The above color changes are interpreted to be a result of regional, secular redox variations generally related to sedimentation rate. A similar, but very general, secular trend is evident at Sites 306 and 1213 (Fig. F4), although poor-age control and stratigraphic uncertainties render precise intersite correlations difficult. The upper Albian chert and porcellanite recovered are brownish in hue, followed downcore by a shift to greenish black hues in the upper Albian at both sites. Toward the base of the Albian sections and persisting down through the upper Aptian, more oxidizing conditions prevailed based on the reddish brown lithologies. The transition to more greenish black colors occurs in the lower Aptian, and at Site 1214 the inferred reducing conditions persist to the bottom of the cored interval (Hauterivian), whereas at Site 1213, the color changes to reddish brown in the lower part of the Berriasian and remains this way through the bottom of the cored interval.

Significant intervals of early Campanian- to Barremian-aged chert/porcellanite also were recovered at Site 1207, and Santonian- through Valanginian-aged chert/porcellanite at Site 305. Site 1207 downcore color trends are much less pronounced relative to the distinctive trends in chert/porcellanite color found at Sites 1213 and 1214. The less distinct redox-controlled rock color trends at Site 1207 may be related to greater downhole contamination of chert fragments. However, some evidence of a secular trend in redox conditions can be gleaned from the record for comparison with the Southern High of Sites 1213 and 1214 (Fig. F4). General coincidence of lithologic color, and by inference prevailing redox conditions of Sites 1207, 1213, and 1214, occurs in the mid- to lower Cenomanian to upper Albian (oxidizing), the middle portion of the Albian (reducing), the lower Albian to upper Aptian (oxidizing), and the lower Aptian to upper Barremian (reducing).

The changes in regional redox chemistry recorded in the chert and porcellanite intervals may reflect changes in the sedimentation rates (see Fig. F6). Generally higher sedimentation rates correspond to sedimentary intervals that record more reducing conditions (typically greenish black lithologies), whereas slower sedimentation rates permit greater oxidation of the sediments, which thus retain more reddish brown colors induced by the oxidation of Fe oxides. These subtle changes do not necessarily indicate less oxygenated deep water because higher sedimentation rates can drive pore water redox conditions toward the more reducing end-member. In fact, the sedimentation rate-redox condition relationship breaks down at Sites 1207 and 1214. Site 1207 sedimentation rates were constant throughout the Cretaceous (8.7 m/m.y.), despite significant and somewhat systematic variation in lithologic color throughout the cored interval. At Site 1214, relatively high sedimentation rates of 12.7 m/m.y. characterize the Albian interval, coincident with the broad occurrence of grayish black lithologies. But sed-

F4. Plot of chert and porcellanite color vs. age, ODP Sites 1207, 1213, and 1214, as well as DSDP Sites 305 and 306, p. 21.



imentation rates within and below the lower Albian are low (<3.7 m/m.y.), despite an interval of grayish black lithology spanning much of the Aptian-aged material recovered. Thus, it is likely that secular changes in prevailing redox conditions were driven by a combination of organic matter flux, overall sedimentation rate, and deepwater oxygen level. However, there may be a hiatus spanning the Barremian and part of the Hauterivian, and the slow sedimentation rates cited above could be artifacts of this missing interval.

BIOSTRATIGRAPHY

Site 1214 yielded sediments of Neogene to Hauterivian age. The Neogene section consisted of a thin veneer of upper Pleistocene foraminiferal sands. A major unconformity separates this layer from underlying upper Albian sedimentary rocks. These sedimentary rocks primarily consist of cherts, with occasional layers of limestone and porcellanite. Sedimentation rates were relatively high throughout the Albian and Aptian. Nannofossil and radiolarian biostratigraphy suggests that at least the upper to middle portion of OAE1a was recovered in Core 198-1214A-23R. Below this interval, sediment accumulation rates decrease in the Barremian and Hauterivian.

Calcareous nannofossils are generally abundant and moderately preserved in Hole 1214A. Planktonic foraminifers are poorly preserved in both the Neogene and Cretaceous samples and few in number in the Cretaceous. Samples in the Cretaceous were commonly scraped from ooze or chalk on chert pieces.

Studies of benthic foraminifers were conducted on a few samples from Hole 1214A. They are common and well preserved in the Neogene but are poorly preserved and exhibit low abundances in the Cretaceous section. Stratigraphic ranges of benthic foraminifers are summarized in Table T3.

Radiolarians were examined from only one sample (Sample 198-1214A-23R-1, 47–49 cm) and are generally well preserved.

Calcareous Nannofossils

Calcareous nannofossils are generally abundant and moderately to well preserved throughout the section in Hole 1214A (Table T4). The section comprises a single core of upper Pleistocene overlying an Albian to Hauterivian sequence that is missing most or all of the Barremian. With the exception of the Pleistocene core, recovery was limited to chert pieces, porcellanite, and small pieces of chalk, and most nannofossil samples were scraped from the soft ooze/chalk on chert pieces. Almost all favorable lithologies were sampled, and all cores yielded nannofossils.

Pleistocene

The Pleistocene is represented only in Section 198-1214A-1R-CC and contains *Pseudoemiliana lacunosa* and *Gephyrocapsa parallela*, indicating Subzone CN14a.

T3. Cenozoic and Cretaceous benthic foraminifers, Hole 1214A, p. 28.

T4. Calcareous nannofossil datums, ages, and depths, p. 29.

Cretaceous

The Cretaceous section ranges from the upper Albian (lower Subzone NC10a) to Hauterivian (Zone NC4). The uppermost Cretaceous sample (Sample 198-1214A-2R-CC) contains *Eiffellithus turriseiffelii* and *Staurolithites glaber*, indicating the lower part of upper Albian Subzone NC10a. A condensed section or unconformity may exist in the middle Albian, as suggested by the co-occurrence of the FOs of *E. turriseiffelii*, *Eiffellithus monechiae*, and *Tranolithus orionatus*. With that exception, the Albian section is biostratigraphically complete.

An organic-rich and noncalcareous interval was recovered toward the base of the Aptian section in Core 198-1214A-23R, and nannofossil biostratigraphy suggests that this correlates to Zone NC6, which supports the correlation of this interval with OAE1a. The green porcellanites and claystones were barren of nannofossils, but a siliceous limestone piece at the bottom of the core (Sample 198-1214A-23R-1, 120–122 cm) yields the lowest downhole occurrence (i.e., FO) of *Hayesites irregularis*, marking the base of Zone NC6 (lower Aptian). The core below, Core 198-1214A-24R, contains *Crucellipsis cuvillieri* and *Calcicalathina oblongata*, indicating Hauterivan Zone NC4. Samples from Core 198-1214A-24R also contain very abundant *Micrantholithus* fragments and rare nannoconids and present something of a paleoecological/paleobiogeographic conundrum, as these taxa have not been recorded from stratigraphically comparable sediments recovered at Site 1213.

Planktonic Foraminifers

The sequence cored in Hole 1214A comprises a single core of upper Pleistocene sediments overlying a Lower Cretaceous sequence. The planktonic foraminifers in the Pleistocene sample (Sample 198-1214A-1R-CC) are poorly preserved and are characterized by selective dissolution and fragmentation (Table T5). The assemblage is dominated by *Globorotalia inflata* and *Truncorotalia crassaformis*. This sample is assigned to Zone N22 based on the presence of few *Truncorotalia truncatulinoides* and *Truncorotalia tosaensis*.

In the underlying Lower Cretaceous sequence, which mainly consists of chert and porcellanite with rare interbedded limestone, planktonic foraminifers are generally few in number and poorly preserved. Planktonic foraminifers were observed in only a few samples obtained by scraping the relatively soft chalk or limestone from the chert cobbles. Samples 198-1214A-2R-1, 0–9 cm, to 4R-1, 0–17 cm, yield moderately preserved uppermost Albian planktonic foraminifers, including few *Hedbergella delrioensis*, *Hedbergella almadenensis*, *Hedbergella simplex*, *Hedbergella planispira*, *Costellagerina libyca*, *Globigerinelloides bentonensis*, *Globigerinelloides ultramicrus*, *Heterohelix moremani*, and *Ticinella roberti*. This interval is assigned to the *Rotalipora appenninica* Zone (KS16) based on the presence of rare specimens of the nominal taxon. Poorly preserved assemblages are present in Samples 198-1214A-5R-1, 19–23 cm, to 7R-1, 2–4 cm, which contain rare *Ticinella primula*, *Hedbergella delrioensis*, and *G. bentonensis*. The presence of *Biticinella breggiensis* in Sample 198-1214A-9R-1, 8–11 cm, permits the identification of the *B. breggiensis* Zone (KS14). The underlying interval from Samples 198-1214A-10R-1, 13–15 cm, to 16R-1, 29–30 cm, belong to the *T. primula* Zone (KS13). The presence of very small hedbergellids from Samples 198-1214A-17R-1, 27–28 cm, to 19R-1, 35–36 cm, is indicative of the *Hedbergella planispira* Zone (KS12). Sample 198-1214A-20R-1, 23–24 cm, is as

T5. Planktonic foraminifer datums, ages, and depths, p. 30.

signed to the *Ticinella bejaouaensis* Zone (KS11) (late Aptian) based on the presence of few *Ticinella bejaouaensis* and *Hedbergella trocoidea*. No planktonic foraminifers were observed in Core 198-1214A-23R, which contains a noncalcareous and organic-rich interval correlated with the lower Aptian Selli horizon (OAE1a). In the oldest core recovered in Hole 1214A, the presence of *Hedbergella sigali*, "*H. delrioensis*," and *Globigerinelloides* sp. in the absence of leupoldinids and clavishedbergellids indicates the Hauterivian *Hedbergella sigali*–"*H. delrioensis*" Zone.

Benthic Foraminifers

Benthic foraminifers were examined in selected samples (Table T3). They are well preserved and common in abundance in the Neogene but are generally poorly preserved (some are completely replaced by silica) and rare in abundance in the Cretaceous.

Paleodepth estimates are based on the work of Pflum and Frerichs (1976), Woodruff (1985), and van Morkhoven et al. (1986) for the Neogene section. For the Cretaceous section, estimates are mainly based on the studies of Kaiho (1998), Holbourn et al. (2001), and backtracked paleodepth curves from the DSDP and Ocean Drilling Program (ODP) data of Kaiho (1999).

Neogene

The only Pleistocene sample examined (Sample 198-1214A-1R-CC) contains a benthic assemblage similar to those observed at other Shatsky Rise sites, represented by *Cibicidoides wuellerstorfi*, *Gyroidinoides girardanus*, *Oridorsalis umbonatus*, *Pyrgo* spp., abundant *Uvigerina hispida*, and *Uvigerina hispidocostata*. This assemblage is indicative of upper abyssal depths (2000–3000 m).

Cretaceous

Because of poor core recovery, all samples were scraped from the edges of indurated lithologies. In Samples 198-1214A-2R-1, 0–9 cm, through 5R-1, 19–23 cm (uppermost Albian), benthic assemblages are generally represented by *Protosangularia albiana*, *Dentalina* spp., *Nodosaria* spp., and abundant agglutinated species (*Dorothia gradata*, *Gaudryina dividens*, *Marssonella praeoxycona*, and *Spiroplectinella excolata*). In addition to these benthic foraminifers, Sample 198-1214A-7R-1, 4–6 cm, contains a diverse benthic assemblage including *Conorotalites aptiensis*, abundant *Gyroidinoides infracretaceus*, *Hanzawaia compressa*, *Pleurotomella* spp., *Spiroplectammia* sp., and *Pseudoclavulina* sp. In Samples 198-1214A-9R-1, 9–11 cm, through 19R-1, 35–37 cm (upper Albian–lower Aptian), benthic assemblages are represented by *Gyroidinoides infracretaceus*, *Protosangularia albiana*, *Dentalina* spp., *Dorothia conula*, and *G. dividens*. *Buliminella* spp. are also present in Samples 198-1214A-16R-1, 28–29 cm, and 19R-1, 35–37 cm. *Lenticulina* spp., one of the characteristic groups in the Lower Cretaceous at other Shatsky Rise sites, has a sporadic presence and very low abundances at Site 1214. Aptian Sample 198-1214A-22R-1, 32–33 cm, contains very poorly preserved *Gavelinella* spp. and *Gyroidinoides infracretaceus*. Samples 198-1214A-23R-1, 54–66 cm, through 23R-1, 93–94 cm, from the OAE1a interval contain no benthic foraminifers. Sample 198-1214A-25R-1, 19–21 cm, (early Hauterivian) contains *Gavelinella intermedia*, *Buliminella* spp., and *Marssonella praeauteriviana*.

Holbourn et al. (2001) assign a “middle–lower bathyal (1000–2000 m)” depth for benthic foraminiferal assemblages dominated by diverse nodosariids, rotaliids, and agglutinated taxa with calcareous cements. Upper Albian–Aptian benthic assemblages observed at Site 1214 are generally similar to this “middle–lower bathyal” assemblage but lack the diverse nodosariids, probably because of poor preservation and the small sample size examined. Furthermore, the presence of *Protosanguularia albiana* in this interval, one of the characteristic taxa in the Early to mid-Cretaceous, indicates depths of ~1500–2500 m (lower bathyal–uppermost abyssal), according to Kaiho (1998, 1999).

Radiolarians

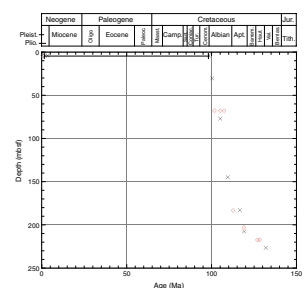
One sample was examined in Hole 1214A to help constrain the age of green and black claystones and porcellanites in Core 198-1214A-23R that were characterized by the absence of other microfossils. Well-preserved radiolarians were found in Sample 198-1214A-23R-1, 47–49 cm, taken from the greenish gray clay interval between the thin tuff layers (see “**Lithostratigraphy**,” p. 4). This sample is characterized by the presence of *Archaeodictyomitra excellens* (Tan), *Archaeodictyomitra* (?) *lacrimula* (Foreman), *Archaeodictyomitra chalilovi* (Aliev), *Cryptamphorella clivosa* (Aliev), *Eucyrtis micropora* (Squinabol), *Pseudodictyomitra carpatica* (Loznyiak), *Pseudodictyomitra lanceoloti* (Schaaf), *Pseudodictyomitra leptoconica* (Foreman), *Sethocapsa* (?) *orca* (Foreman), *Syringocapsa* sp. cf. *Stylosphaera coronata* Steiger sensu Erbacher (1994), *Thanarla conica* (Aliev), *Thanarla pulchra* (Squinabol), and *Wrangellium puga* (Schaaf). There are many nassellarian species in this sample, and dominant genera include *Archaeodictyomitra*, *Pseudodictyomitra*, *Sethocapsa*, *Thanarla*, and *Cryptamphorella*. Baumgartner et al. (1995) report that *P. carpatica* ranges from Zone UAZ11 to Zone UAZ21 (Late Jurassic to Barremian). However, more recent studies by Premoli Silva et al. (1999) suggest that this species occurs in the Selli level (early Aptian) in Italy, thereby extending its range. Furthermore, the radiolarian assemblage of this sample does not contain the genera *Pantanellium* or *Podobursa*. The last occurrences (LOs) of these genera have been reported by Erbacher and Thurow (1997) to lie in the lowermost part of the Selli level. Therefore, this assemblage indicates an age of late early Aptian and suggests that these sediments were deposited during the middle to upper part of the OAE1a.

SEDIMENTATION AND ACCUMULATION RATES

Unconformities and changes in sedimentation rate at Site 1214 are illustrated in a plot of calcareous microfossil datum ages (first and last occurrences) vs. depth (Fig. F5). These rates rely on major calcareous nannofossil and planktonic foraminiferal datums presented in Tables T4 and T5 (see “**Biostratigraphy**,” p. 9). The Pleistocene–Hauterivian section cored at Site 1214 is punctuated by one major unconformity separating the Pleistocene and uppermost Albian.

Core 198-1214A-1R contains <1 m of Pleistocene sediment. The remainder of the cored interval is Early Cretaceous in age and is characterized by poor recovery of chert-bearing chalk, limestone, and porcellanite. Despite the poor recovery, all cores contain datable calcareous nannofossil assemblages that were supported by planktonic foraminifers and/or radiolarians (see “**Biostratigraphy**,” p. 9). The uppermost

F5. Age-depth plot of calcareous nannofossil and planktonic foraminiferal datums, p. 22.



Aptian–Albian interval accumulated at an average rate of 12.7 m/m.y. The interval from near OAE1a in the lower Aptian through the upper Aptian accumulated at a reduced rate of 3.7 m/m.y. The basal Aptian–Hauterivian is either missing at Site 1214 or is represented by an unrecovered condensed interval (sedimentation rates of ~1.3 m/m.y.), which is consistent with trends observed at Site 1213 (Fig. F6).

ORGANIC GEOCHEMISTRY

Carbonate and Organic Carbon

Carbonate determinations by coulometry were made for a total of six samples from Hole 1214A (Table T6). Samples were chosen to provide a measure of the carbonate content in Albian limestones from Subunit IIB. Elemental concentrations of C, H, N, and S were also measured (Table T6) for three samples from the lower Aptian (Subunit IID) to assess the enrichment of organic matter in discrete intervals. Two samples (198-1214A-23R-1, 20–22 cm, and 87–89 cm) taken from darker horizons interbedded with green claystones proved lean in organic matter (0–0.1 wt%). The contents of organic carbon are higher (1.4 wt%) in a clayey porcellanite (Sample 198-1214A-23R-1, 5–7 cm), though lower than the enriched values found in the lower Aptian at Sites 1207 and 1213 (Tables T12, p. 128, in the “Site 1207” chapter and T11, p. 102, in the “Site 1213” chapter).

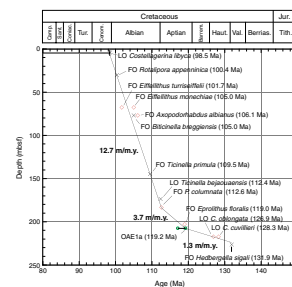
Assessment of Extractable Hydrocarbons and Ketones

Hydrocarbon compositions were examined in the lower Aptian sample (198-1214A-23R-1, 5–7 cm) containing elevated organic carbon contents (>1 wt%) (Table T6) to characterize the biological sources and thermal maturity of its organic matter. In addition, comparison of biomarker distributions with other lower Aptian C_{org}-rich intervals can help assess the depositional conditions that led to enhanced sequestration of organic matter. The procedure followed the methodology described in “Organic Geochemistry,” p. 18, in the “Explanatory Notes” chapter. In addition, gas chromatography–mass spectrometry (GC-MS) was used to examine the composition of CH₂Cl₂ eluates from the silica separation step of the samples consisting primarily of ketones.

Examination of the lower molecular weight hydrocarbons was precluded by the presence of significant contaminant hydrocarbons from petroleum products, but the polycyclic steroid and hopanoid hydrocarbons could be evaluated. Components were identified from responses at specific target intervals in individual ion chromatograms and from their mass spectra. All of the hydrocarbons are well documented as components of mid-Cretaceous black shales (e.g., Barnes et al., 1979; Rullkötter et al., 1984, 1987; Farrimond et al., 1986b, 1990; Simoneit, 1986; Simoneit and Stuermer, 1982). There are fewer published identifications of ketones in sediments of this age (Comet et al., 1981; Farrimond et al., 1986a).

The patterns of distributions of the hydrocarbons and ketones (Table T7; Fig. F7) are broadly similar to those observed at Sites 1207 and 1213. Among the hydrocarbons, the prominence of Δ⁴- and Δ⁵-sterenes derived from eukaryotic sterols is more reminiscent of Site 1207, although none of the bacterial methylhopanoids observed in the C_{org}-rich intervals at that site are present. The distribution pattern of steroi-

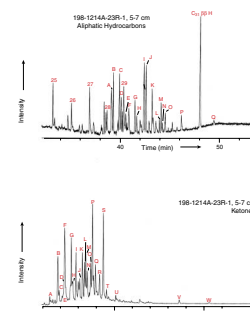
F6. Age-depth plot of Early Cretaceous calcareous nannofossil and planktonic foraminiferal datums, with radiolarians from a single Aptian sample, p. 23.



T6. Carbonate and elemental composition, p. 31.

T7. Aliphatic hydrocarbons and ketone identities, p. 32.

F7. GC-MS trace of aliphatic hydrocarbons and ketones, p. 24.



dal ketones closely resembles that found in Hole 1213B, but the distinctive components derived from various bacterial sources (cf. Table T14, p. 105, in the “Site 1213” chapter) are absent. Thus, the uniformity in characteristics attributable to algal primary producers over the region of Shatsky Rise provides a stark contrast to the restricted occurrence of critical bacterial markers, notably methylhopanoids. However, it is also important to emphasize that the limited recovery means that Sample 198-1214A-23R-1, 5–7 cm, is probably not representative of the episode of maximum sequestration of organic matter during OAE1a at Site 1214. The close resemblance of its polycyclic hydrocarbon distribution to the leanest interval at Site 1207 (Sample 198-1207B-44R-1, 103–104 cm) supports this assessment. These considerations reinforce the interpretation that the depositional conditions that led to accumulation of horizons containing >10% of C_{org} were clearly exceptional and suggest that they promoted bacterial processes that otherwise were of minor significance.

PHYSICAL PROPERTIES

Physical properties at Site 1214 were measured on both whole-round sections and discrete samples from split-core sections. Because of poor core recovery, only one core section was measured on the multisensor track (MST). The MST records of magnetic susceptibility and gamma ray attenuation (GRA) bulk density thus only represent the Pleistocene interval. Discrete measurements of compressional P -wave velocity were made at a routine frequency of at least one measurement per split-core section from Hole 1214A. No index properties measurements were made.

MST Measurements

Whole-round Core 198-1214A-1R was measured on the MST for magnetic susceptibility and GRA bulk density at 3-cm intervals. No P -wave or natural gamma radiation measurements were made with the MST. The collected MST data are archived in the ODP Janus database.

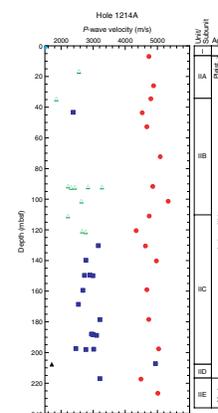
Hole 1214A magnetic susceptibility values appear to display no discernible downhole trend, although these data are comparable with values measured in the Pleistocene interval at other Leg 198 sites (see “MST Measurements,” p. 37, in “Physical Properties” in the “Site 1207” chapter; “MST Measurements,” p. 29, in “Physical Properties” in the “Site 1208” chapter; “MST Measurements,” p. 29, in “Physical Properties” in the “Site 1209” chapter; “MST Measurements,” p. 27, in “Physical Properties” in the “Site 1210” chapter; “MST Measurements,” p. 25, in “Physical Properties” in the “Site 1211” chapter; and “MST Measurements,” p. 23, in “Physical Properties” in the “Site 1212” chapter). GRA bulk density data show a slight downhole increase between the seafloor and ~1.25 mbsf.

P -Wave Velocity

Discrete measurements of compressional P -wave velocity were made on Site 1214 split-core sections using the modified Hamilton Frame (PWS3) velocimeter. These data are listed in Table T8 and illustrated in Figure F8. Data were collected at a routine sampling frequency of at least one measurement per section. A variety of lithologies were cored

T8. Discrete measurements of P -wave velocity, p. 33.

F8. P -wave velocities for discrete samples, p. 25.



at Site 1214, each of which has distinct *P*-wave velocities (Table T9). Within the recovered sediments, a general downhole increase in *P*-wave velocity between 0 and ~220 mbsf is most likely related to progressive sediment lithification with increasing burial depth.

Summary

Physical properties data from Site 1214 primarily reflect compositional variability between the different sediments recovered. Data from the recovered sediments are diagnostic both of the depth of burial (i.e., degree of lithification) and also the amount of silicification. The high degree of variability of *P*-wave velocities below 90 mbsf, which is related to lithology, has significant implications for seismic interpretations of Site 1214 and related stratigraphic sections.

T9. *P*-wave velocities for lithologies, p. 34.

REFERENCES

- Barnes, P.J., Brassell, S.C., Comet, P., Eglinton, G., McEvoy, J., Maxwell, J.R., Wardroper, A.M.K., and Volkman, J.K., 1979. Preliminary lipid analysis of core sections 18, 24, and 30 from Hole 402A. *In* Montadert, L., Roberts, D.G., et al., *Init. Repts. DSDP*, 48: Washington (U.S. Govt. Printing Office), 965–976.
- Baumgartner, P.O., Bartolini A., Carter, E.S., Conti, M., Cortese, G., Danelian, T., De Wever, P., Dumitrica, P., Dumitrica-Jud, R., Gorican, S., Guex, J., Hull, D.M., Kito, N., Marcucci, M., Matsuoka, A., Murchev, B., O'Dogherty, L., Savary, J., Vishnevskaya, V., Widz, D., and Yao, A., 1995. Middle Jurassic to Early Cretaceous radiolarian biochronology of Tethys based on unitary associations. *In* Baumgartner, P. O., O'Dogherty, L., Gorican, S., Urquhart, E., Pillevuit, A., and De Wever, P. (Eds.), *Middle Jurassic to Lower Cretaceous Radiolaria of Tethys: Occurrences, Systematics, Biochronology*. Mem. Geol. (Lausanne), 23:1013–1048.
- Comet, P.A., McEvoy, J., Brassell, S.C., Eglinton, G., Maxwell, J.R., and Thomson, I.D., 1981. Lipids of an Upper Albian limestone, Deep Sea Drilling Project Site 465, Section 465A-38-3. *In* Thiede, J., Vallier, T.L., et al., *Init. Repts. DSDP*, 62: Washington (U.S. Govt. Printing Office), 923–937.
- Erbacher, J., and Thurow, J., 1997. Influence of oceanic anoxic events on the evolution of mid-Cretaceous radiolaria in the North Atlantic and western Tethys. *Mar. Micropaleontol.*, 30:139–158.
- Farrimond, P., Eglinton, G., and Brassell, S.C., 1986a. Alkenones in Cretaceous black shales, Blake-Bahama Basin, western North Atlantic. *In* Leythaeuser, D., and Rullkötter, J. (Eds.), *Advances in Organic Geochemistry, 1985*. Org. Geochem., 10:897–903.
- , 1986b. Geolipids of black shales and claystones in Cretaceous and Jurassic sediment sequences from the North American Basin. *In* Summerhayes, C.P., and Shackleton, N.J. (Eds.), *North Atlantic Palaeoceanography*. Spec. Publ.—Geol. Soc. London, 21:347–360.
- Farrimond, P., Eglinton, G., Brassell, S.C., and Jenkyns, H.C., 1990. The Cenomanian/Turonian anoxic event in Europe: an organic geochemical study. *Mar. Pet. Geol.*, 7:75–89.
- Holbourn, A., Kuhnt, W., and Soeding, E., 2001. Atlantic paleobathymetry, paleoproductivity and paleocirculation in the late Albian: the benthic foraminiferal record. *Palaeogeogr., Palaeoclimatol., Palaeoecol.*, 170:171–196.
- Kaiho, K., 1998. Phylogeny of deep-sea calcareous trochospiral benthic foraminifera: evolution and diversification. *Micropaleontology*, 44:291–311.
- , 1999. Evolution in the test size of deep-sea benthic foraminifera during the past 120 million years. *Mar. Micropaleontol.*, 37:53–65.
- Larson, R.L., Moberly, R., et al., 1975. *Init. Repts. DSDP*, 32: Washington (U.S. Govt. Printing Office).
- Pflum, C.E., and Frerichs, W.E., 1976. Gulf of Mexico deep-water foraminifera. *Spec. Publ.—Cushman Found. Foraminiferal Res.*, 14:1–122.
- Premoli Silva, I., Erba, E., Salvini, G., Locatelli, C., and Verga, D., 1999. Biotic changes in Cretaceous oceanic anoxic events of the Tethys. *J. Foraminiferal Res.*, 29:352–370.
- Rullkötter, J., Mukhopadhyay, P.K., and Welte, D.H., 1984. Geochemistry and petrography of organic matter in sediments from Hole 530A, Angola Basin, and Hole 532, Walvis Ridge, Deep Sea Drilling Project. *In* Hay, W.W., Sibuet, J.-C., et al., *Init. Repts. DSDP*, 75 (Pt. 2), Washington (U.S. Govt. Printing Office), 1069–1087.
- , 1987. Geochemistry and petrography of organic matter from Deep Sea Drilling Project Site 603, lower continental rise off Cape Hatteras. *In* van Hinte, J.E., Wise, S.W., Jr., et al., *Init. Repts. DSDP*, 93 (Pt. 2): Washington (U.S. Govt. Printing Office), 1163–1176.

- Simoneit, B.R.T., 1986. Biomarker geochemistry of black shales from Cretaceous oceans—an overview. *Mar. Geol.*, 70:9–41.
- Simoneit, B.R.T., and Stuermer, D.H., 1982. Organic geochemical indicators for sources of organic matter and paleoenvironmental conditions in Cretaceous oceans. In Schlanger, S.O., and Cita, M.B. (Eds.), *Nature and Origin of Cretaceous Carbon-Rich Facies*: New York (Academic Press), 145–163.
- Sliter, W.V., 1989. Aptian anoxia in the Pacific Basin. *Geology*, 17:909–912.
- , 1992. Cretaceous planktonic foraminiferal biostratigraphy and paleoceanographic events in the Pacific Ocean with emphasis on indurated sediment. In Ishizaki, K., and Saito, T. (Eds.), *Centenary of Japanese Micropaleontology*: Tokyo (Terra Sci.), 281–299.
- Sliter, W.V., and Brown, G.R., 1993. Shatsky Rise: seismic stratigraphy and sedimentary record of Pacific paleoceanography since the Early Cretaceous. In Natland, J.H., Storms, M.A., et al., *Proc. ODP, Sci. Results*, 132: College Station, TX, (Ocean Drilling Program), 3–13.
- Thierstein, H.R., 1979. Paleoceanographic implications of organic carbon and carbonate distribution in Mesozoic deep sea sediments. In Talwani, M., Hay, W.W., and Ryan, W.B.F. (Eds.), *Deep Drilling Results in the Atlantic Ocean: Maurice Ewing Ser.*, Am. Geophys. Union, 3:249–274.
- van Morkhoven, F.P.C.M., Berggren, W.A., and Edwards, A.S., 1986. Cenozoic cosmopolitan deep-water benthic foraminifera. *Bull. Cent. Rech. Explor.—Prod. Elf-Aquitaine*, 11.
- Woodruff, F., 1985. Changes in Miocene deep-sea benthic foraminiferal distribution in the Pacific Ocean: relationship to paleoceanography. In Kennett, J.P. (Ed.), *The Miocene Ocean: Paleoceanography and Biogeography*. Mem.—Geol. Soc. Am., 163:131–175.

Figure F1. Core recovery, lithology, lithologic units, and age with corresponding biostratigraphic zonations. Lith. = lithology, foram. zn. = foraminiferal zone, nanno. zn. = nannofossil zone, rad. zn. = radiolarian zone.

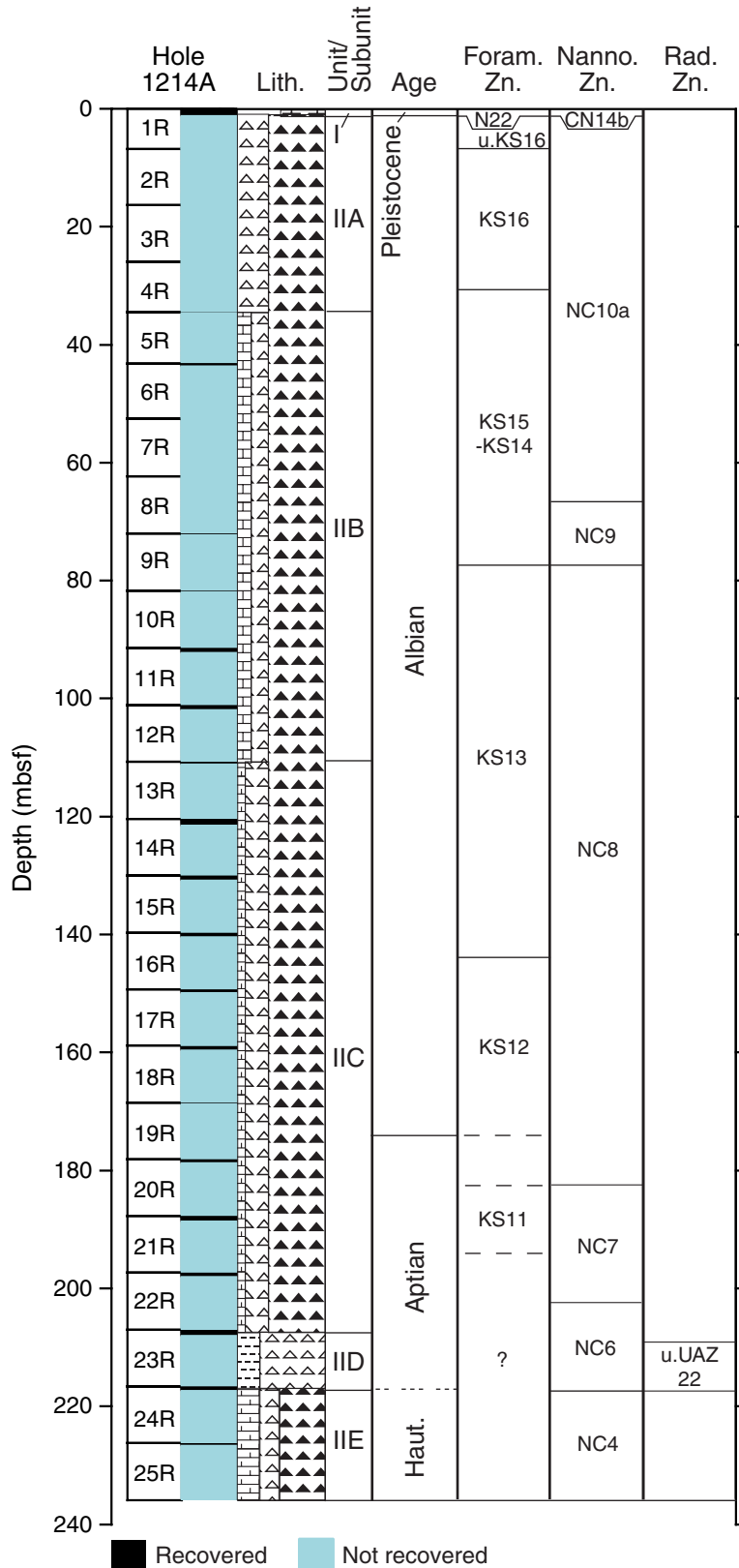


Figure F2. Composite digital photograph of Section 198-1214A-23R-1, which contains the sedimentary sequence spanning the lower Aptian Oceanic Anoxic Event (OAE1a). The red arrows indicate the location of layers that may be altered tuff deposits.

Core
1214A-23R-1

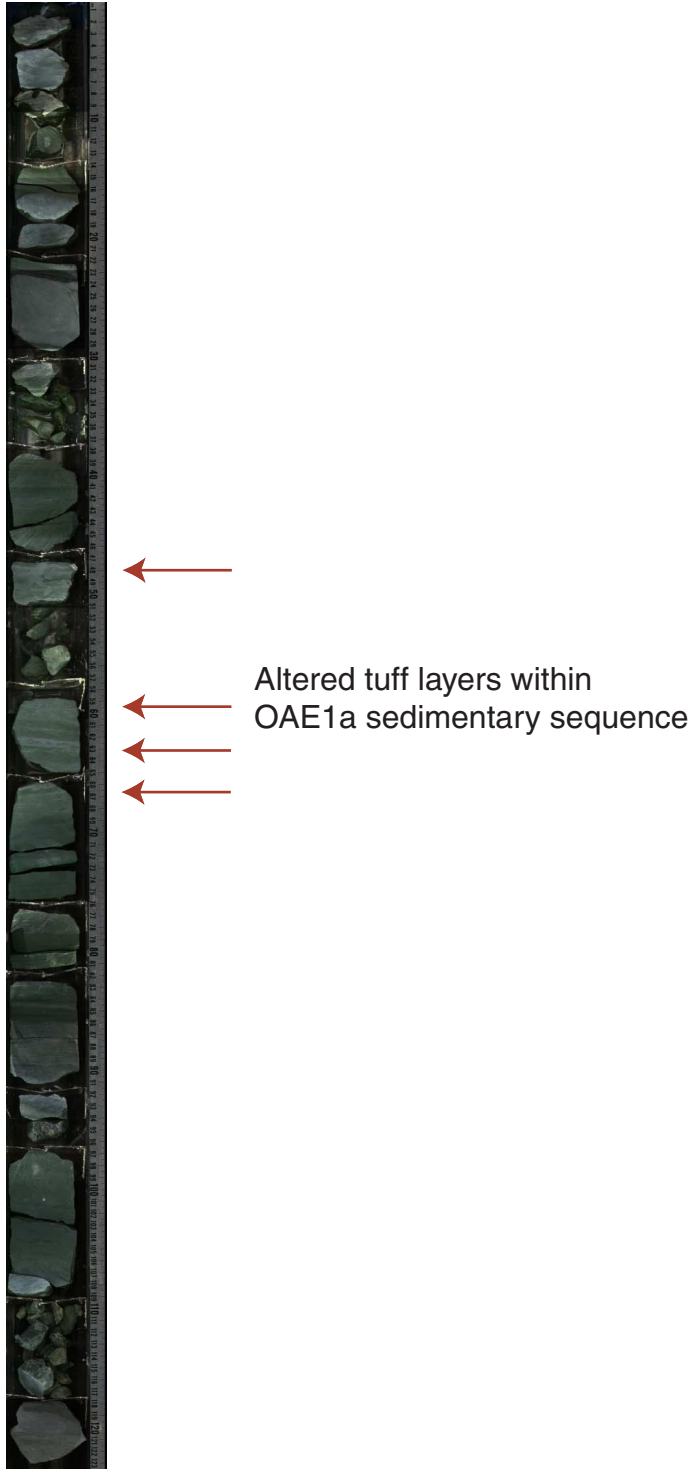


Figure F3. Close-up digital photograph detailing pyrite that has replaced radiolarians from 66 to 69 cm (interval 198-1214A-14R-1, 57–69 cm).

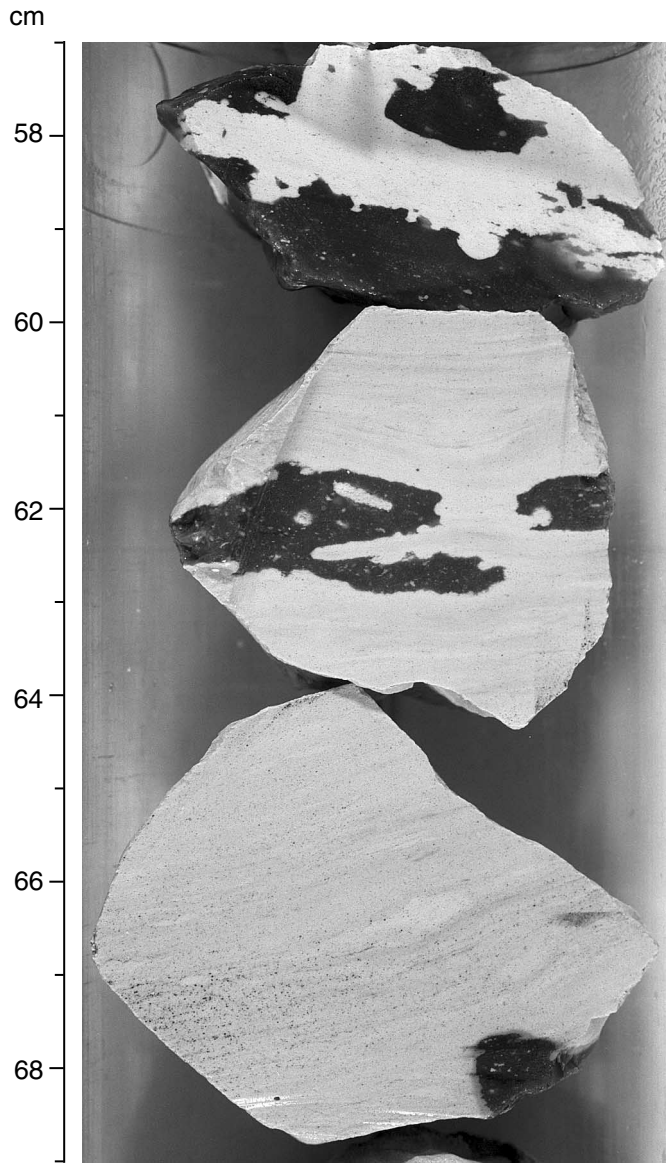


Figure F4. Generalized plot of chert and porcellanite color (either “oxidized” hues [red] or “reduced” hues [black]) vs. age for Sites 1207, 1213, and 1214, as well as DSDP Sites 305 and 306. The age attributions of Sites 305 and 306 were obtained from Sliter (1989, 1992). See Tables T3, p. 119, in the “Site 1207” chapter, T4, p. 95, in the “Site 1213” chapter, and T2, p. 27, for detailed color variation.

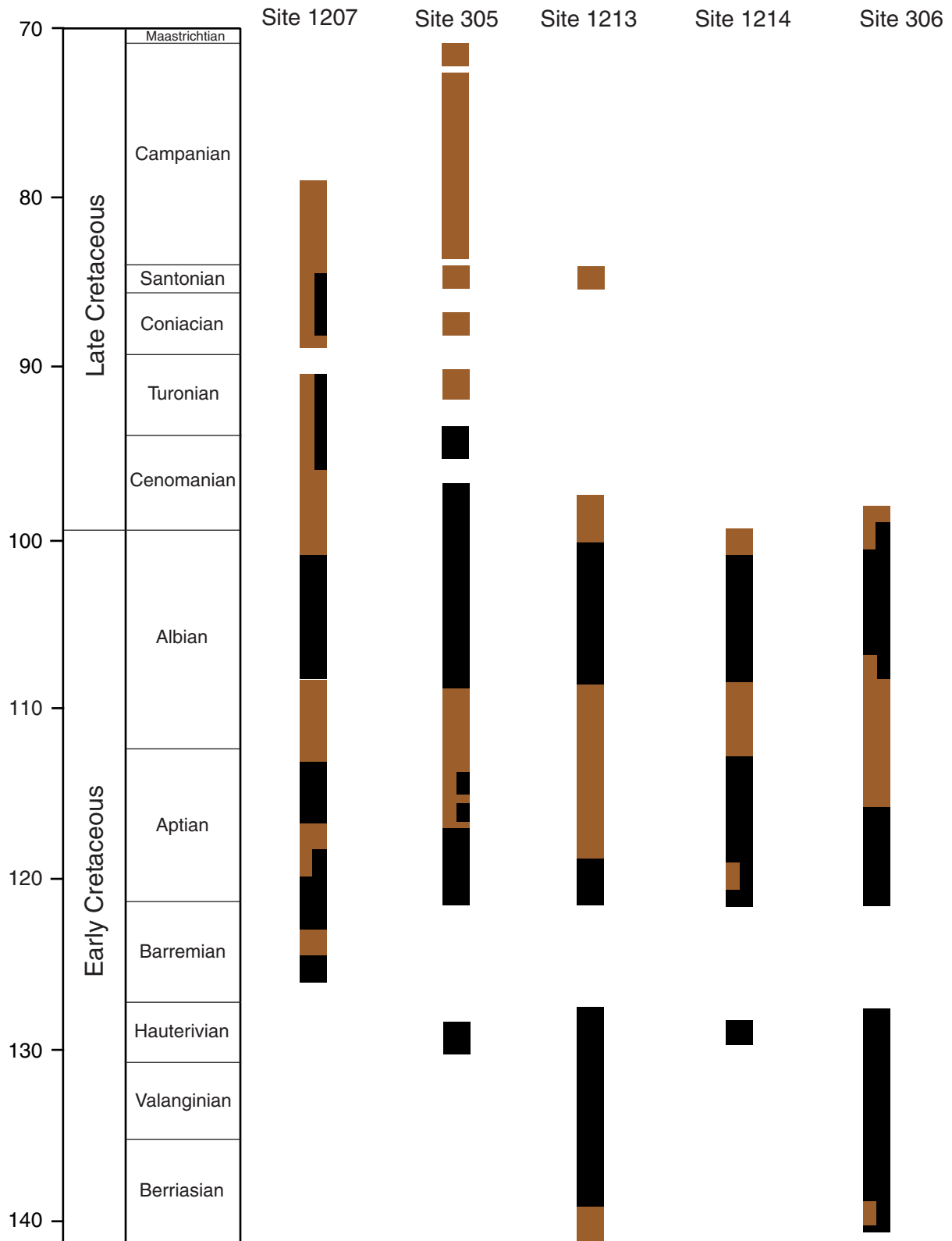


Figure F5. Age-depth plot of calcareous nannofossil (diamonds) and planktonic foraminiferal (crosses) datums at Site 1214. The horizontal line represents the major unconformity in the section (see discussion in "Sedimentation and Accumulation Rates," p. 12). Datum ages and depths are presented in Tables T4, p. 29, and T5, p. 30 (see "Biostratigraphy," p. 9).

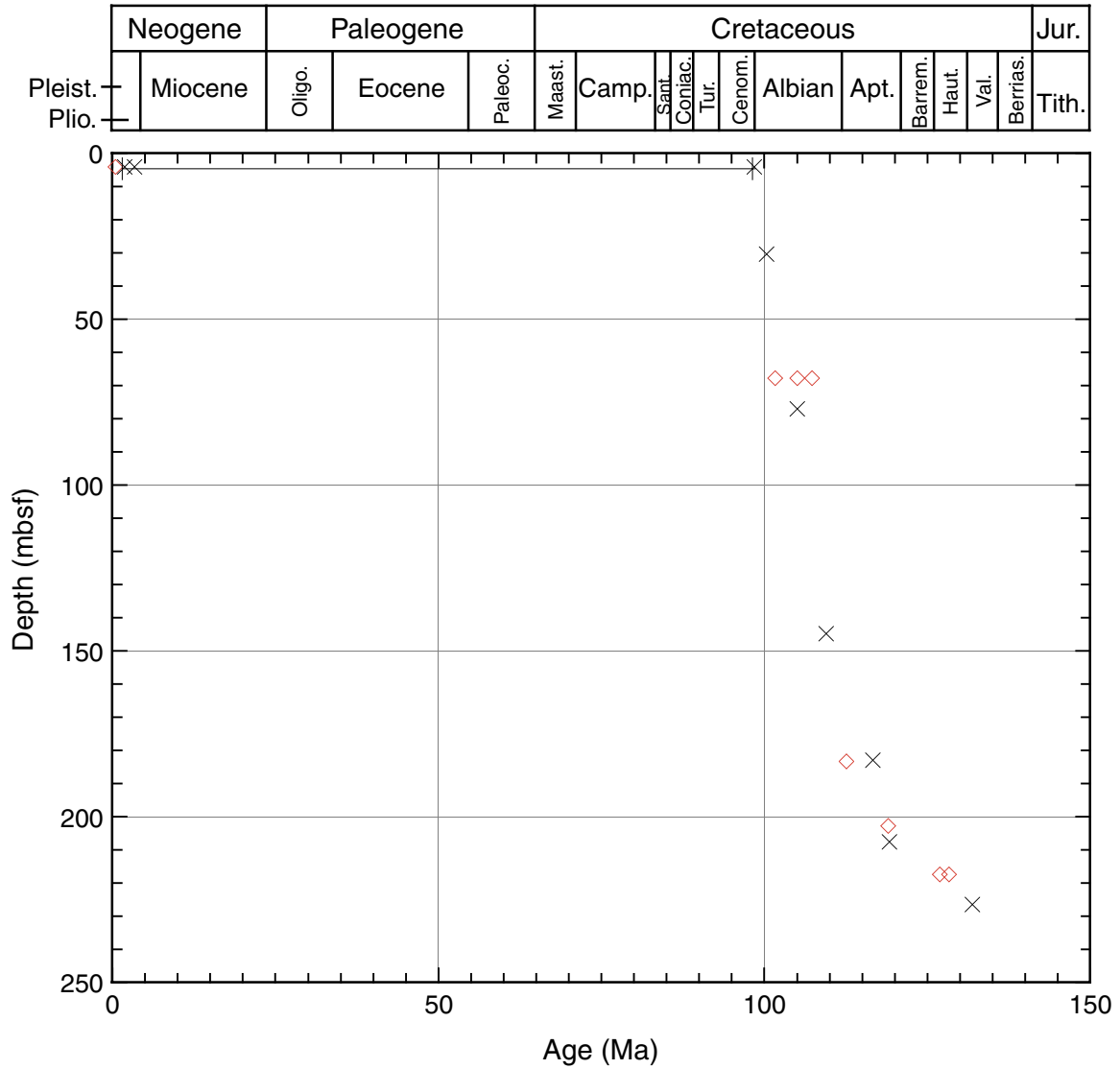


Figure F6. Age-depth plot of Early Cretaceous (latest Albian–Hauterivian) calcareous nannofossil (diamonds) and planktonic foraminiferal (crosses) datums at Site 1214, together with radiolarians from a single Aptian sample (circles connected by a line mark the upper and lower limits of the “upper lower Aptian to upper Aptian” zone). The horizontal line depicts the major unconformity in the section (see discussion in “Sedimentation and Accumulation Rates,” p. 12). Datum ages and depths are presented in Tables T4, p. 29, and T5, p. 30. FO = first occurrence, LO = last occurrence, OAE1a = Aptian Oceanic Anoxic Event.

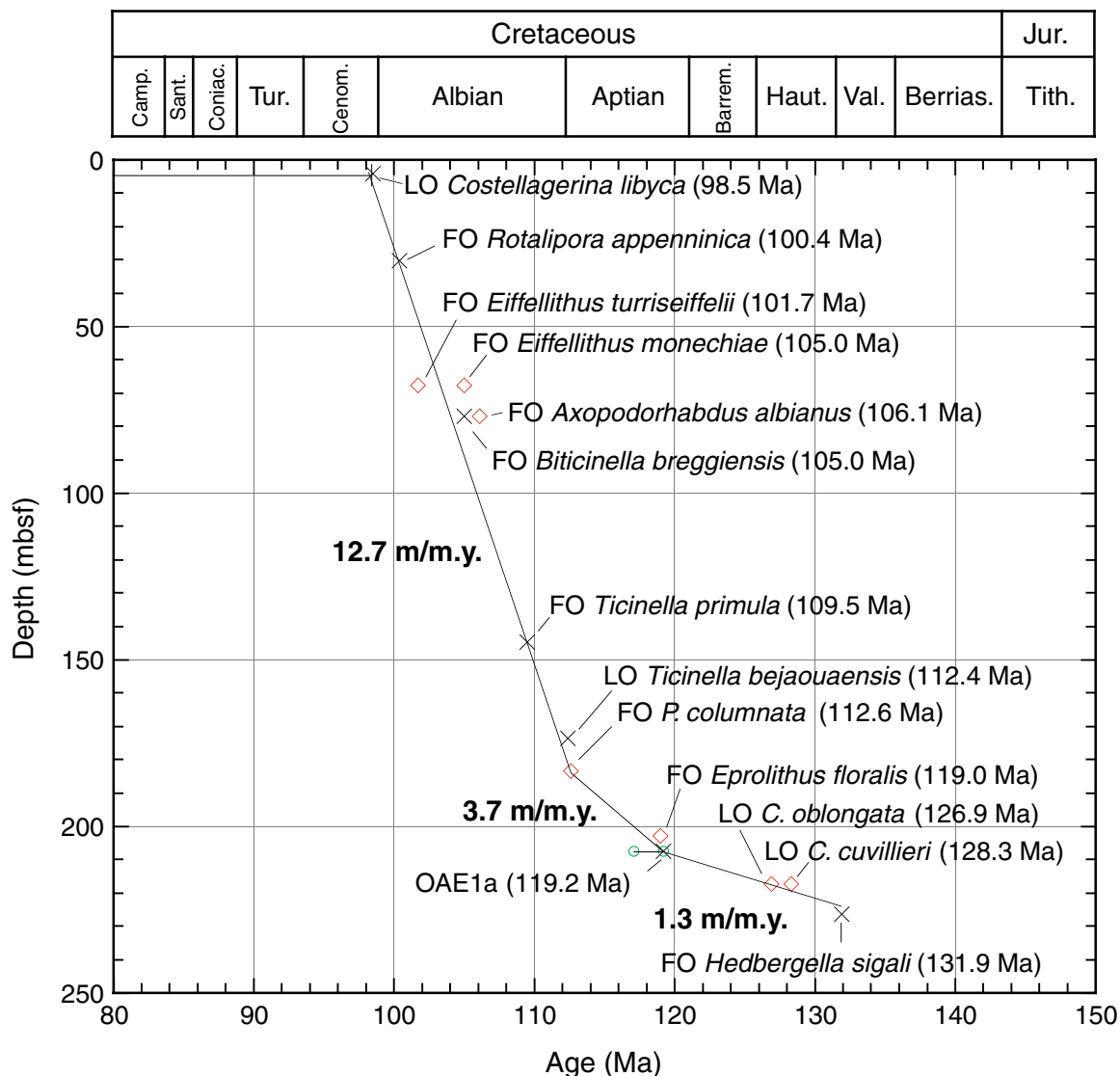


Figure F8. P-wave velocities for discrete samples from Hole 1214A (see Table T8, p. 33, for data). Light blue diamond = ooze, blue squares = porcellanite, open triangle = claystone, green triangles = chalk and limestone, red circles = chert.

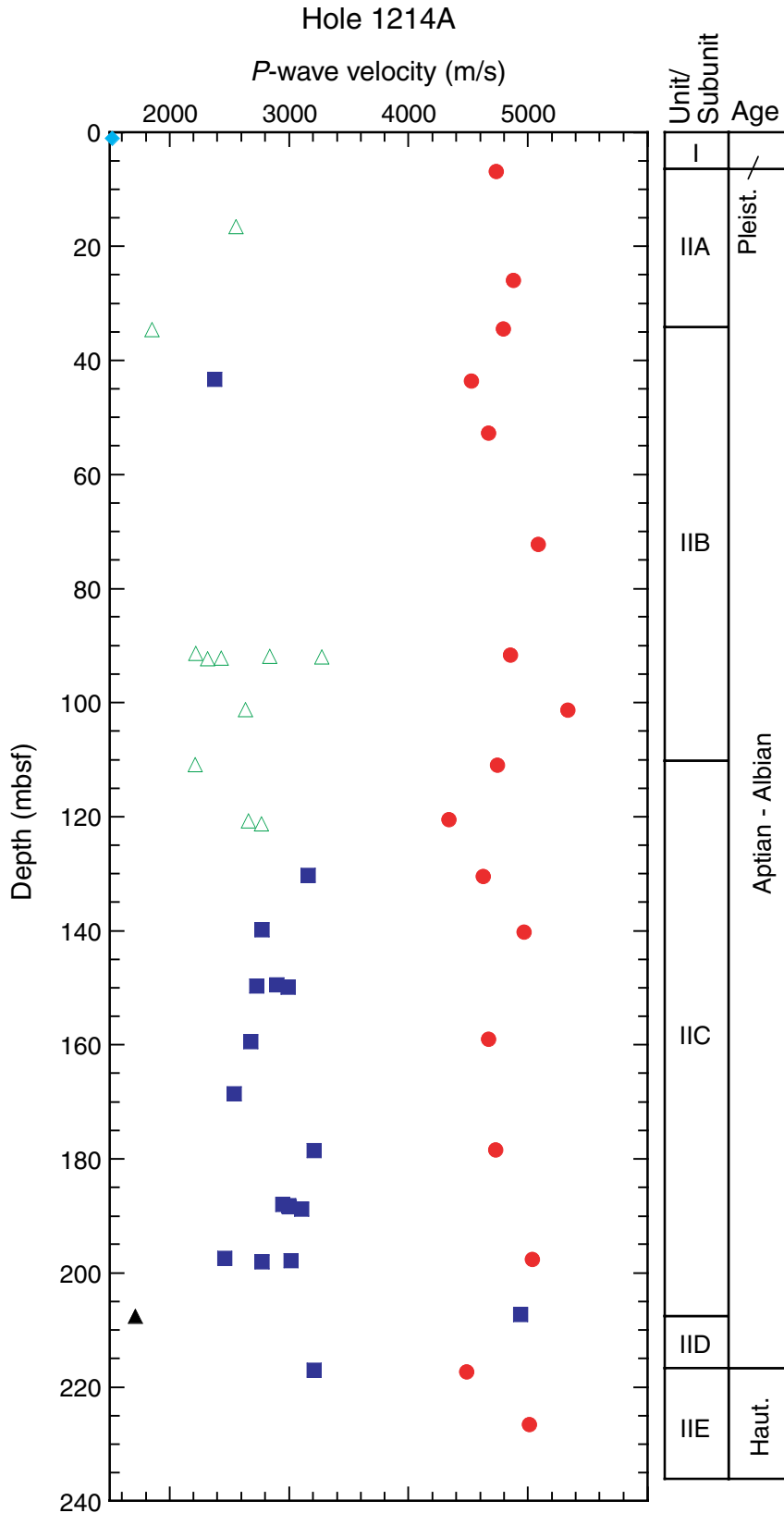


Table T1. Coring summary, Site 1214.

Hole 1214A

Latitude: 31°52.0254'N
 Longitude: 157°28.7178'E
 Time on site (hr): 68.25 (0415 hr, 12 Oct–0030 hr, 15 Oct 2001)
 Time on hole (hr): 68.25 (0415 hr, 12 Oct–0030 hr, 15 Oct 2001)
 Seafloor (drill pipe measurement from rig floor, mbrf): 3413.0
 Distance between rig floor and sea level (m): 11.4
 Water depth (drill pipe measurement from sea level, m): 3401.6
 Total depth (drill pipe measurement from rig floor, mbrf): 3648.9
 Total penetration (mbsf): 235.9
 Total length of cored section (m): 235.9
 Total core recovered (m): 16.49
 Core recovery (%): 6.99
 Total number of cores: 25
 Total number of drilled intervals: 0

Core	Date (Oct 2001)	Local time (hr)	Depth (mbsf)		Length (m)		Recovery (%)
			Top	Bottom	Cored	Recovered	
198-1214A-							
1R	12	1300	0.0	6.9	6.9	1.32	19.10
2R	12	1527	6.9	16.4	9.5	0.09	0.90
3R	12	1730	16.4	25.9	9.5	0.20	2.10
4R	12	1900	25.9	34.5	8.6	0.18	2.10
5R	12	2105	34.5	43.2	8.7	0.20	2.30
6R	12	2250	43.2	52.6	9.4	0.50	5.30
7R	13	0025	52.6	62.3	9.7	0.26	2.70
8R	13	0200	62.3	72.0	9.7	0.09	0.90
9R	13	0345	72.0	81.7	9.7	0.39	4.00
10R	13	0530	81.7	91.4	9.7	0.33	3.40
11R	13	0730	91.4	101.1	9.7	0.95	9.80
12R	13	0905	101.1	110.7	9.6	0.98	10.20
13R	13	1055	110.7	120.4	9.7	0.56	5.80
14R	13	1300	120.4	130.0	9.6	1.29	13.40
15R	13	1500	130.0	139.7	9.7	0.90	9.30
16R	13	1700	139.7	149.3	9.6	0.87	9.10
17R	13	1930	149.3	158.8	9.5	0.77	8.10
18R	13	2115	158.8	168.5	9.7	0.91	9.40
19R	13	2255	168.5	178.1	9.6	0.36	3.80
20R	14	0040	178.1	187.7	9.6	0.79	8.20
21R	14	0305	187.7	197.3	9.6	1.08	11.20
22R	14	0520	197.3	207.0	9.7	0.80	8.20
23R	14	0805	207.0	216.6	9.6	1.20	12.50
24R	14	1010	216.6	226.2	9.6	0.88	9.20
25R	14	1145	226.2	235.9	9.7	0.59	6.10
Cored totals:					235.9	16.49	6.99

Table T4. Calcareous nannofossil datums, ages, and depths, Site 1214.

Datum	Zone/ Subzone (base)	Core, section, interval (cm)	Depth (mbsf)	Age (Ma)
		198-1214-		
FO <i>Gephyrocapsa parallela</i>	CN14a	1R-CC	1.27	0.95
LO <i>Staurolithites glaber</i>		2R-1, 1	6.90	97.5
FO <i>Eiffellithus turriseiffelii</i>	NC10a	8R-1, 1	62.37	101.7
FO <i>Eiffellithus monechiae</i>	NC9b	8R-1, 1	62.37	105.0
FO <i>Axopodorhabdus albianus</i>	NC9a	9R-1, 9-11	72.09	106.1
FO <i>Prediscosphaera columnata</i>	NC8a	20R-1, 23	178.33	112.6
FO <i>Eprolithus floralis</i>	NC7a	22R-1, 72-77	198.02	119.0
LO <i>Calicalathina oblongata</i>	NC5d-e	24R-1, 72-75	217.32	125.1
LO <i>Cruciellipsis cuvillieri</i>	NC5a	24R-1, 72-75	217.32	128.3

Note: FO = first occurrence, LO = last occurrence.

Table T5. Planktonic foraminiferal datums, ages, and depths, Site 1214.

Datum	Zone (base)	Core, section, interval (cm)	Depth (mbsf)	Age (Ma)
		198-1214-A-		
FO <i>Truncorotalia truncatulinoides</i>	N22	1R-CC	1.27	1.92
FO <i>Truncorotalia tosaensis</i>	N21	1R-CC	1.27	3.35
LO <i>Costellagerina libyca</i>		2R-1, 9	6.9	98.5
FO <i>Rotalipora appenninica</i>	KS16	4R-1, 17	25.9	100.4
FO <i>Biticinella breggiensis</i>	KS14	9R-1, 9	72.09	105.0
FO <i>Ticinella primula</i>	KS13	16R-1, 28	139.98	109.5
LO <i>Ticinella bejaouaensis</i>		20R-1, 23	178.33	112.4
FO <i>Hedbergella sigali</i>		25R-1, 19	226.39	131.9

Note: FO = first occurrence, LO = last occurrence.

Table T6. Carbonate content and elemental composition of samples, Hole 1214A.

Core, section, interval (cm)	Depth (mbsf)	Inorganic carbon (wt%)	Carbonate (wt%)	Organic carbon (wt%)	Nitrogen (wt%)	Sulfur (wt%)	Hydrogen (wt%)	C/N ratio (atomic)
198-1214A-								
10R-1, 41-42	82.11	4.9	41.0	ND	ND	ND	ND	NA
11R-1, 92-93	92.32	5.9	49.0	ND	ND	ND	ND	NA
13R-1, 25-26	110.95	4.7	39.2	ND	ND	ND	ND	NA
23R-1, 5-7	207.05	0.1	0.8	1.4	0.08	0.23	0.47	14.8
23R-1, 20-21	207.20	0.1	0.4	0.1	0.01	0.46	0.45	10.7
23R-1, 87-89	207.87	0.1	0.6	0.0	0.00	0.46	0.50	NA

Notes: ND = not determined, NA = not applicable.

Table T7. Identities of aliphatic hydrocarbons and ketones whose peaks are labeled in Figure F7, p. 24.

Peak	Code	Identification
Aliphatic hydrocarbons:		
A	C ₂₇ Δ ⁴ S	Cholest-4-ene
B	C ₂₇ Δ ⁵ S	Cholest-5-ene
C	C ₂₈ Δ ^{4,22} S	24-methylcholesta-4,22-diene
D	C ₂₈ Δ ^{5,22} S	24-methylcholesta-5,22-diene
E	C ₃₀ T	Unknown C ₃₀ triterpene (dammaradiene?)
F	C ₂₇ βH	22,29,30-trisnor-17β(H)-hopane
G	C ₂₉ Δ ^{4,22} S	24-ethylcholest-4,22-diene
H	C ₂₉ Δ ^{5,22} S	24-ethylcholest-5,22-diene
I	C ₂₉ Δ ⁴ S	24-ethylcholest-4-ene
J	C ₂₉ Δ ⁵ S + C ₂₉ Δ ¹⁷⁽²¹⁾ H	24-ethylcholest-5-ene + 30-norhop-17(21)-ene
K	30Δ ¹⁷⁽²¹⁾ H	Hop-17(21)-ene
L	C ₃₀ αβH	17α(H),21β(H)-hopane
M	Δ ⁸ F	Fern-8-ene
N	C ₃₀ Δ ¹³⁽¹⁸⁾ NH	Neohop-13(18)-ene
O	C ₂₉ ββH	30-nor-17β(H),21β(H)-hopane
P	C ₃₀ ββH	17β(H),21β(H)-hopane
C ₃₁ ββH	C ₃₁ ββH	17β(H),21β(H)-homohopane
Q	C ₃₂ ββH	17β(H),21β(H)-bishomohopane
Ketones:		
A	β-T, γ-T	β- and γ-tocopherol
B	U	Unknown
C	C ₂₇ βS	5β(H)-cholestan-3-one
D	C ₂₇ βH	22,29,30-trisnor-17β(H)-hopan-21-one
E	α-T	α-tocopherol
F	C ₂₇ αS	5α(H)-cholestan-3-one
G	C ₂₈ Δ ²² S	24-methylcholest-22-en-3-one
H	ME C ₂₈ S	4-methyl-5α(H)-cholestan-3-one
I	C ₂₇ Δ ⁴ S	Cholest-4-en-3-one
J	C ₂₈ αS	24-methyl-5α(H)-cholestan-3-one
K	C ₂₈ Δ ^{4,22} S	24-methylcholesta-4,22-dien-3-one
L	C ₂₉ Δ ²² S	24-ethylcholest-22-en-3-one
M	C ₂₉ βS	24-ethyl-5β(H)-cholestan-3-one
N	ME C ₂₉ S	4,24-dimethyl-5α(H)-cholestan-3-one
O	ME C ₃₀ Δ ²² S + C ₂₈ Δ ⁴ S	4,23,24-trimethylcholest-22-en-3-one + 24-methylcholest-4-en-3-one
P	C ₂₉ αS	24-ethyl-5α(H)-cholestan-3-one
Q	C ₂₉ Δ ^{4,22} S	24-ethylcholest-4,22-dien-3-one
R	ME C ₃₀ ETS	4-methyl-24-ethyl-5α(H)-cholestan-3-one
S	C ₂₉ Δ ⁴ S	24-ethylcholest-4-en-3-one
T	C ₃₀ T + ME C ₃₁ Δ ²² S	C ₃₀ triterpenone + 4,23-dimethyl-24-ethylcholest-22-en-3-one
U	C ₃₀ ββH	17β(H),21β(H)-hopanone
V	C ₃₃ ββH	17β(H),21β(H)-trishomohopan-32-one
W	C ₃₄ ββH	17β(H),21β(H)-tetrakishomohopan-33-one

Table T8. Discrete measurements of *P*-wave velocity, Site 1214.

Core, section, interval (cm)	Depth (mbsf)	Velocity (m/s)
198-1214A-		
1R-1, 107	1.06	1522.2
2R-1, 6	6.96	4735.0*
3R-1, 14	16.54	2557.6*†
4R-1, 13	26.03	4878.4*
5R-1, 4	34.54	4796.2*
5R-1, 12	34.62	1853.0†
6R-1, 12	43.32	2376.4‡
6R-1, 43	43.63	4524.9*
7R-1, 12	52.72	4672.1*
9R-1, 30	72.30	5084.8*
11R-1, 4	91.44	2217.9†
11R-1, 23	91.63	4855.9*
11R-1, 48	91.88	2839.1†
11R-1, 65	92.05	3274.5†
11R-1, 80	92.20	2430.1†
11R-1, 96	92.36	2318.1†
12R-1, 12	101.22	2636.0†
12R-1, 24	101.34	5332.8*
13R-1, 19	110.89	2217.2†
13R-1, 31	111.01	4743.7*
14R-1, 16	120.56	4338.6*
14R-1, 35	120.75	2658.9†
14R-1, 88	121.28	2769.9†
15R-1, 31	130.31	3161.0‡
15R-1, 46	130.46	4629.8*
16R-1, 10	139.80	2776.6‡
16R-1, 59	140.29	4967.7*
17R-1, 16	149.46	2900.0‡
17R-1, 40	149.70	2729.7‡
17R-1, 57	149.87	2990.1‡
18R-1, 20	159.00	4672.7*
18R-1, 62	159.42	2679.2‡
19R-1, 13	168.63	2538.8‡
20R-1, 37	178.47	4728.6*
20R-1, 48	178.58	3211.8‡
21R-1, 31	188.01	2948.8‡
21R-1, 48	188.18	2996.2‡
21R-1, 69	188.39	3000.1‡
21R-1, 106	188.76	3104.6‡
22R-1, 18	197.48	2463.9‡
22R-1, 34	197.64	5037.2*
22R-1, 52	197.82	3019.4‡
22R-1, 77	198.07	2773.4‡
23R-1, 26	207.26	4940.5‡
23R-1, 61	207.61	1713.0**
24R-1, 52	217.12	3210.8‡
24R-1, 75	217.35	4488.5*
25R-1, 36	226.56	5010.3*

Note: * = chert, † = chalk or limestone, ‡ = porcellanite, ** = claystone.

Table T9. *P*-wave velocities for the lithologies recovered at Site 1214.

Lithology	Velocity (m/s)		
	Minimum	Mean	Maximum
Seafloor sediment	NA	1522.2	NA
Claystone	NA	1713.0	NA
Chalk and limestone	1853.0	2524.6	3274.5
Porcellanite	2376.4	2990.1	4940.5
Chert	4338.6	4794.0	5332.8

Note: NA = not available.